Near-GeV Acceleration of Electrons by a Nonlinear Plasma Wave Driven by a Self-Guided Laser Pulse

S. Kneip,[1] S. R. Nagel,[1] S. F. Martins,[2] S. P. D. Mangles,[1] C. Bellei,[1] O. Chekhlov,[3] R. J. Clarke,[3] N. Delerue,[4] E. J. Divall,[3] G. Doucas,[4] K. Ertel,[3] F. Fiuza,[2] R. Fonseca,[2] P. Foster,[3] S. J. Hawkes,[3] C. J. Hooker,[3] K. Krushelnick,[1,5] W. B. Mori,[6] C. A. J. Palmer,[1] K. Ta Phuoc,[7] P. P. Rajeev,[3] J. Schreiber,[1] M. J. V. Streeter,[3] D. Urner,[4] J. Vieira,[2] L. O. Silva,[2] and Z. Najmudin[1]

[1]*The Blackett Laboratory, Imperial College London, London, SW7 2BZ, United Kingdom*
[2]*GoLP/Instituto Plasmas e Fusão Nuclear, Instituto Superior Técnico, Lisbon, Portugal*
[3]*Central Laser Facility, Rutherford Appleton Laboratory, Oxon, OX11 0QX, United Kingdom*
[4]*The John Adams Institute, Department of Physics, University of Oxford, Oxford, OX1 3RH, United Kingdom*
[5]*Center for Ultrafast Optical Science, University of Michigan, Ann Arbor, Michigan, 48109, USA*
[6]*Department of Physics and Astronomy and Department of Electrical Engineering, UCLA, Los Angeles, California, 90095, USA*
[7]*Laboratoire d'Optique Appliquée, ENSTA, Ecole Polytechnique, Palaiseau, 91761, France*

(Received 18 February 2009; published 16 July 2009; publisher error corrected 16 July 2009)

The acceleration of electrons to $\simeq 0.8$ GeV has been observed in a self-injecting laser wakefield accelerator driven at a plasma density of 5.5×10^{18} cm^{-3} by a 10 J, 55 fs, 800 nm laser pulse in the blowout regime. The laser pulse is found to be self-guided for 1 cm ($>10 z_R$), by measurement of a single filament containing $>30\%$ of the initial laser energy at this distance. Three-dimensional particle in cell simulations show that the intensity within the guided filament is amplified beyond its initial focused value to a normalized vector potential of $a_0 > 6$, thus driving a highly nonlinear plasma wave.

DOI: 10.1103/PhysRevLett.103.035002 PACS numbers: 52.38.Kd, 41.75.Jv, 52.38.Hb

Recent advances in plasma based particle acceleration have demonstrated energy gain in excess of GeV [1,2]. In the laser wakefield (LWF) scheme [3], the accelerating field is generated by the ponderomotive force of an intense laser. When driven to a large enough amplitude, the wakefield can trap and accelerate electrons from the plasma, due to wave breaking [4]. It has been shown that self-injected electrons can be accelerated to almost the same energy, leading to beams with comparatively low energy spread [5–7]. When guided in an optical waveguide, a plasma accelerator driven by a high intensity laser has demonstrated a gain of $\simeq 1$ GeV over 3.3 cm [2].

For densities less than the critical density ($n_e \ll n_c$), the wakefield has a phase velocity just less than the speed of light c, with a relativistic factor $\gamma_{\rm ph} \simeq \omega_0/\omega_p$, equal to the ratio of the laser and plasma frequency. As the electrons are accelerated, they rapidly exceed $\gamma_{\rm ph}$ and eventually outrun the wave. Thus, the electrons cease to be accelerated after a dephasing length, $L_d \simeq \gamma_{\rm ph}^2 \lambda_p$, where $\lambda_p = 2\pi c/\omega_p$. For a three-dimensional nonlinear wake in the blowout regime, the maximum energy gain due to dephasing is $W_{\rm max} \simeq \frac{2}{3} a_0 (n_c/n_e)$ [8], where a_0 is a measure of the laser intensity $a_0 \propto \sqrt{I}$. Hence, energy gain *increases* with decreasing plasma density, mainly because the dephasing length ($\propto n_e^{-3/2}$) also increases.

The dephasing length is typically longer than the Rayleigh length, z_R, the length over which the laser defocuses in vacuum. In case of a Gaussian pulse $z_R \simeq \pi w_0^2/\lambda_0$, with laser wavelength λ_0. For a laser spot diameter $2w_0 \simeq \lambda_p$, which is close to ideal for the blowout regime [8,9], then $z_R \propto n_e^{-1}$. Hence, by going to lower density, to obtain a higher final energy, the ratio $L_d/z_R \simeq \omega_0/(\pi\omega_p) = \gamma_{\rm ph}/\pi$ increases. So, even if a laser pulse is intense enough to inject electrons into a wakefield, there is no guarantee that it can accelerate them sufficiently far to achieve maximum energy gain.

Therefore, some form of optical guiding is required to ensure acceleration over a dephasing length. It has been commonly thought that self-guiding for the short pulses required for LWF acceleration is not possible due to a cancellation of relativistic and ponderomotive terms [10]. Therefore, the use of plasma waveguides has been explored [2,11,12]. However, experiments without plasma channels have also demonstrated acceleration close to the dephasing length [7,9]. In these experiments, the plasma density was relatively high ($n_e \geq 10^{19}$ cm^{-3}) so the acceleration was over $\simeq 2$ mm and $a_0 \simeq 1$, leading to energy gains $\simeq 0.1$ GeV and a complicated laser evolution and injection process. Even for these short dephasing distances ($L_d \simeq 0.1$ mm), despite the cancellation of effects at the front of the laser, sufficient self-guiding does occur. This is due to a combination of relativistic and ponderomotive modification of the refractive index when $P/P_c > 1$ and $a_0 \geq 2$, where $P_c = 17(n_c/n_e)$ GW. For sufficiently large a_0, a nearly spherical wake structure [13] is formed, often referred to as a plasma bubble [14]. For properly matched beams, this bubble can trap the bulk of the laser while the leading edge diffracts slowly as it loses energy to the wake [8,9,14].

For acceleration to higher energies with a self-guided pulse, lower densities are required to extend the dephasing

length. This not only increases the power needed for self-focusing ($P_c \propto n_e^{-1}$), but also the laser power required to obtain a threshold a_0 for injection, since the bubble size also increases with decreasing density.

In this Letter, we report on the first experiments performed with self-guided laser driven plasma accelerators using greater than 200 TW laser pulses. We show that at these high powers, self-guiding in the nonlinear wakefield regime can extend the interaction to a distance exceeding the dephasing length even without an external guiding channel (>1 cm $\simeq 13 z_R$). We also show that the maximum observed electron energy rises with increasing acceleration length, up to a maximum of $\simeq$0.8 GeV. These energies are a result of intensity (a_0) amplification of the laser pulse self-guided over such long distances, which in turn generates a highly nonlinearly steepened plasma wave structure.

The experiments were carried out on the Astra Gemini laser system at the Rutherford Appleton Laboratory. Linearly polarized pulses with a central wavelength of $\lambda_0 = 800$ nm, a Gaussian full-width half maximum (FWHM) pulse duration of $\tau = (55 \pm 5)$ fs, and a maximum energy of (11 ± 1) J were focused to a peak intensity of $I = (1.9 \pm 0.2) \times 10^{19}$ W cm^{-2} or $a_0 = 3.9$ with an off-axis parabolic mirror of focal length $f = 3$ m and F number of $F = 20$. The transverse profile of the laser in vacuum yields a focal spot diameter of $2w_{\mathrm{HWHM}} = (22.0 \pm 0.6)$ μm or $w_0 \simeq 19$ μm at $1/e^2$ of intensity. Thus, $z_R = 2Fw_0 \simeq 760$ μm, which was supported by experimental measurements. Typically, (31 ± 2)% of the pulse energy is within the diameter $2w_{\mathrm{HWHM}}$.

The targets were supersonic helium gas jets with varying nozzle diameters of 3, 5, 8, and 10 mm. The density profile measured by interferometry has a FWHM length of (2.7 ± 0.2), (4.1 ± 0.2), (6.8 ± 0.3), and (8.7 ± 0.3) mm for the different nozzles and consists of a central plateau, which is constant to within 10%, and linear gradients at the edges.

The energy spectrum of accelerated electrons was measured with an electron spectrometer based on a dipole electromagnet with circular pole pieces of radius 167 mm [15]. The magnetic field strength was a function of the applied current, with a maximum of 1.15 T. The spectrometer dispersed the beam onto a phosphor screen (Lanex) imaged with a CCD camera. A tracking code using the measured magnetic field map relates the measured beam deflection to energy. The error bar on the energy measurement is given by the finite acceptance angle of the spectrometer entrance (± 4 mrad), which leads to an uncertainty of 50 MeV at 800 MeV. The phosphor screen was cross calibrated with an image plate detector to obtain absolute charge measurements. In the present setup, the dipole magnet has negligible energy focusing and transverse focusing properties in the detection plane.

The resulting electron spectra obtained at a fixed density of $n_e = (5.7 \pm 0.2) \times 10^{18}$ cm^{-3} are shown in Fig. 1. High-energy electron beams of narrow energy spread are produced, whose peak energy W_{max} increases with increasing length. Averaging several hundred shots with the magnet spectrometer turned off, for plasma densities 2–12×10^{18} cm^{-3}, the root mean square beam position was stable to $\simeq$5 mrad. For the highest energy beams, the pointing variation was 4.0 mrad, and the $1/e$ divergence was 3.6 mrad. The 5 and 10 mm nozzle yield a mean beam charge of 30 and 90 pC averaging over shots at different densities, and a peak beam charge of 350 and 550 pC, respectively, at optimum conditions.

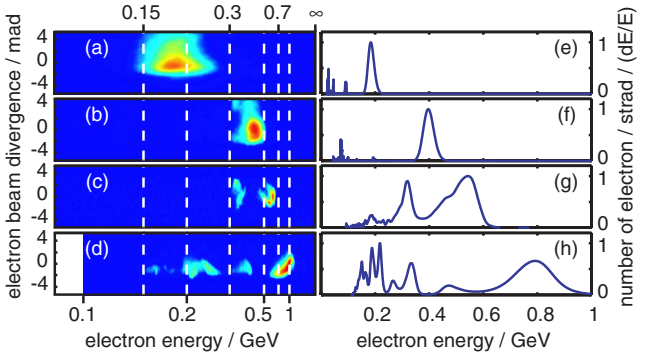

FIG. 1 (color online). Spectrally dispersed electron beams at the exit of the magnetic spectrometer for gas jet lengths (a) 3, (b) 5, (c) 8, and (d) 10 mm, at a plasma density of $n_e = (5.7 \pm 0.2) \times 10^{18}$ cm^{-3} with (10.0 ± 1.5) J of laser energy on target. (e)–(h) Show lineouts of (a) to (d), that have been deconvolved to give the electron number per solid angle and relative energy spread dE/E. All plots are normalized to unity.

The increase of energy with length, shown in Fig. 2 inset, implies two things. First, it suggests that electrons are self-injected early in the interaction. It was found that $a_0 \gtrsim 4.2$ must be satisfied for self-injection [11,16], which compares to our initial $a_0 = 3.9$. Hence, less self-focusing and pulse compression is necessary to increase the laser intensity to that required for injection as compared to previous self-injection experiments performed with $a_0 \simeq 1$ [5–7]. This reduced pulse evolution before injection is also supported by observation of an electron beam on every shot under optimum conditions. Second, the rate of energy gain with length implies a lower accelerating field than in previous experiments at both higher [17] and comparable densities [18]. As described below, this is an indication of complex dynamics within the nonlinear wake, rather than a lower electric field. In fact, the electric field actually increases due to nonlinear steepening of the plasma wave.

Evidence for nonlinear steepening can be seen in Fig. 2, which shows the maximum, W_{max}, and mean observed beam energies W_{mean} as a function of plasma density. We find that W_{max} for the 5 mm ([red] squares) and 10 mm nozzle ([blue] circles) and W_{mean} for the 10 mm nozzle (dashed [blue] line) increase with decreasing density ($W \propto n_e^{-1}$) down to a certain density threshold, below which there is no self-injection. This threshold is close to the density at which the matched spot size is no longer smaller than the vacuum focal spot size so that there is no intensity

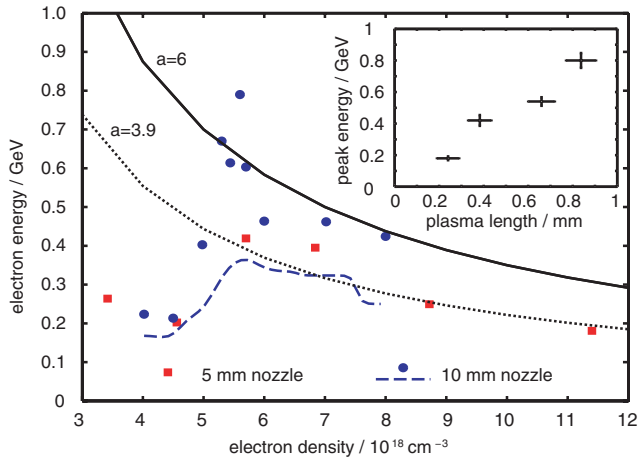

FIG. 2 (color online). Scaling of electron beam energy as a function of plasma density. The maximum achievable peak energy for the 5 mm ([red] squares) and 10 mm nozzle ([blue] circles) and the average peak energy for the 10 mm nozzle (dashed [blue] line) are plotted for (10.0 ± 1.5) J on target. The dotted [black] and solid [black] lines show the predictions by the nonlinear scaling law [8] for $a \simeq 3.9$ and $a \simeq 6.0$. The rms energy stability is 40% and 15% for the 10 mm nozzle at 5.7 and 6.3×10^{18} cm^{-3} averaging over 14 and 7 shots, respectively. (inset) Maximum observed electron energy as a function of plasma length. Error bars are explained in the text.

amplification due to self-focusing. The mean and peak energies for the 5 mm nozzle and the mean beam energy for the 10 mm nozzle above this threshold are predicted by the nonlinear scaling model [8] for $a_0 = 3.9$, close to our average vacuum laser strength. However, the maximum $W_{\max}$ is fitted by a higher $a_0 \simeq 6.0$. This indicates that for ideal guiding, the wakefield amplitude is increased due to the effects of pulse evolution and intensity amplification.

Intensity (a_0) amplification should occur because of pulse compression [19] and photon deceleration [20], as well as self-focusing [9]. Evidence for this intensity amplification is seen by the multiple lower energy electron bunches observed at long interaction lengths [e.g., Figs. 1(c) and 1(d)]. Monoenergetic beam production in a self-injecting laser wakefield can be aided by the fact that continuous injection is inhibited by a reduction of the plasma wave amplitude by the space-charge field of electrons that have already been injected. A bunch can thus be localized in space and, consequently, as the electrons are accelerated by almost the same fields, also in phase space. Intensity amplification means that the plasma wave amplitude also continues to rise, allowing further injection. The bunches which are injected when the wakefield amplitude has increased due to the intensity amplification experience a larger wake amplitude and thus can be accelerated to higher energies. Of course, for this to be possible, the laser pulse must be self-guided over multiple z_R.

Figure 3 depicts multiple views of the laser propagation through the plasma. Interferometry [Fig. 3(a)] shows a plasma channel whose size is increasing at an angle similar to that of the $F = 20$ focusing optic used. Figures 3(d) and 3(e) shows the beam profile after transmission through 10 mm of plasma at high intensity. The profiles show a central bright spot comparable in size to the initial beam focus [Fig. 3(b)], with an outer halo that is comparable to the laser beam profile when the laser is propagated in vacuum [Fig. 3(c)]. We believe the expanding plasma cone is produced by the unguided halo, but there is a central guided filament which propagates at sufficiently high intensity to drive a large amplitude plasma wave. Figures 3(d)–3(h) highlight that self-guiding becomes less effective for decreasing laser powers. Measurements of the transmitted energy with a calibrated diode show that there is typically 30% energy transmission at the end of the interaction, and that half of this transmitted energy is in the central spot (of $2w_0 = 22\ \mu\text{m} \simeq \lambda_p$). We calculate that there is $P \simeq 5$ TW within the guided central filament for conditions shown in Fig. 3(f). This compares favorably with the value of P_c for this threshold density.

For the 10 mm nozzle, particle in cell simulations were performed with parameters matching experimental values with OSIRIS [21]. Results are for a three-dimensional simulation of a linearly polarized, diffraction limited laser pulse with $a_0 = 3.9$ focused at the entrance of the plasma. The longitudinal profile of the laser electric field is symmetric and given by $10\tau^3 - 15\tau^4 + 6\tau^5$, with $\tau = (t - t_0)/\tau_{\text{FWHM}}$, and $\tau_{\text{FWHM}} = 55$ fs. The transverse profile of the laser is Gaussian with $2w_{\text{HWHM}} = 22\ \mu$m. The plasma density profile increases linearly from zero to $n_e = 5.7 \times 10^{18}$ cm^{-3} in the first 650 μm, is constant for 7317 μm, and falls linearly to zero in 1180 μm. In the transverse direction, n_e falls linearly from the center to 5.1×10^{18} cm^{-3} at the edges of the box. The simulation

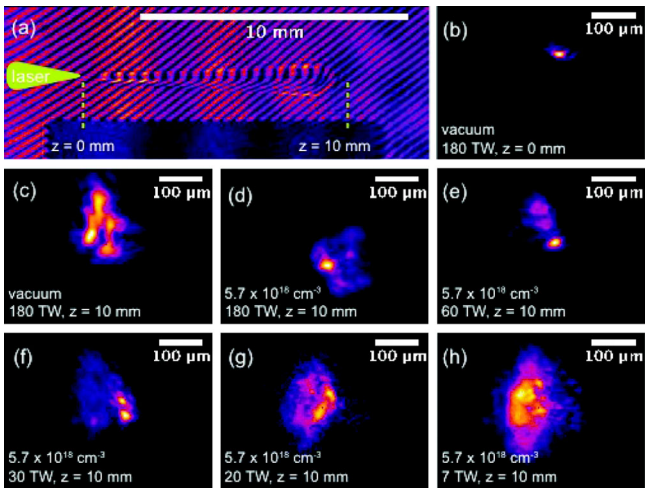

FIG. 3 (color online). (a) Typical interferogram obtained by transverse probing. (b)–(h) background subtracted 2D images of the laser mode for various conditions: (b) in vacuum at the position of optimal focus $z = 0$; (c) in vacuum at $z = 10$ mm; (d)–(h) at $z = 10$ mm with plasma $n_e = (5.7 \pm 0.2) \times 10^{18}$ cm^{-3} and input laser powers of: (d) 180 TW, (e) 60 TW, (f) 30 TW, (g) 20 TW, and (h) 7 TW.

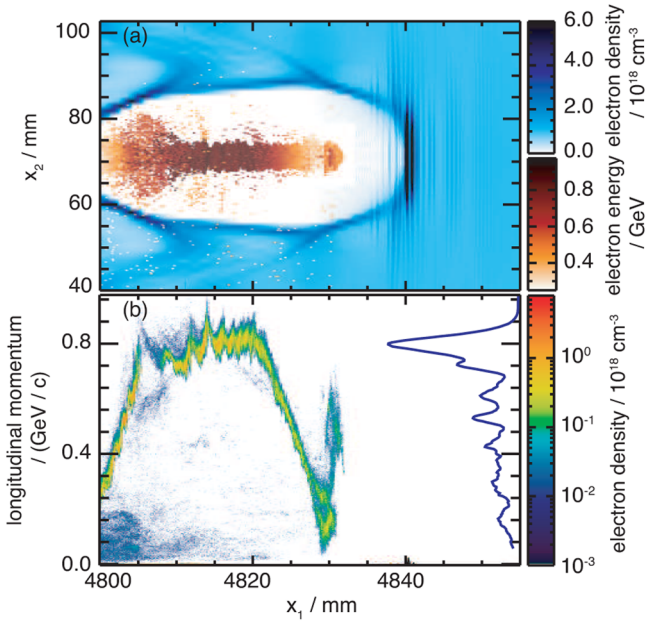

FIG. 4 (color online). Simulation for the density profile of the 10 mm nozzle at $n_e = 5.5 \times 10^{18}$ cm^{-3} (a) plasma density (blue) and injected bunch energy (red); (b) longitudinal momentum of injected electrons. Lineout (right axis) gives corresponding energy spectrum (arb. units).

window is $71 \times 143 \times 143$ μm^3, and follows the laser. A total of 2.3×10^8 particles were pushed for 5×10^5 iterations (1 week computing time on a 256 node cluster). The resolution in the laser propagation direction z is $k_0 \Delta z = 0.16$, and $k_p \Delta x = k_p \Delta y = 0.25$ in the transverse directions.

Figure 4 shows the accelerating structure after a distance of 4.8 mm. The laser pulse has been self-guided over this distance and drives a highly nonlinear plasma wave. The plasma wave self-injects early in the simulation, and there is strong beam loading due to the injected electrons. The acceleration occurs in two phases. The electron bunch at the head of the injected beam is rapidly accelerated to $\simeq$500 MeV and is then decelerated as it dephases. As the laser propagates, the rear self-focuses and the head is continually being self-amplified due to temporal compression. This results in a continual stream of injection, and a large number of electrons is injected into the bubble. Also because of the increasing plasma wave amplitude, electrons which are injected later can attain higher energies than those injected early in the interaction [13]. At the time shown in Fig. 4, the secondary bunch has phase rotated, leading to a narrow energy spread feature in the electron spectrum at 0.8 GeV. The maximum energy gain is due to the combination of beam loading, dephasing, and laser depletion in the accelerating structure. At later times, however, there is little further gain in electron energy, and an electron beam at close to the maximum energy exits the plasma. The simulation predicts a_0 amplification and self-guiding over the full range of the gas jet as deduced from the experimental measurements and explains the maximum energy observed remarkably well, even though the pulse evolution seems to be faster than in the experiment. Because of the continual injection, the total charge of trapped electrons increases with increasing plasma length up to 0.5 nC, which is in excellent agreement with the dependence on length and total charge observed experimentally.

In conclusion, these studies demonstrate that a guiding structure is not essential for laser wakefield acceleration to GeV levels using simple gas jet targets. This open geometry also allows access for advanced injection schemes [18,22] and for harnessing plasma waves as radiation sources [23,24]. This could have a major impact on the uses of GeV electron beams, making them more compact, economical, and prevalent.

The authors wish to acknowledge A. E. Dangor for fruitful discussions and N. Bourgeois, T. Ibbotson, S. Hooker, and the staff of the Central Laser Facility for their assistance during the experiment. S. Kneip acknowledges the Euroleap network for financial assistance.

[1] I. Blumenfeld *et al.*, Nature (London) **445**, 741 (2007).
[2] W. P. Leemans *et al.*, Nature Phys. **2**, 696 (2006).
[3] T. Tajima *et al.*, Phys. Rev. Lett. **43**, 267 (1979).
[4] A. Modena *et al.*, Nature (London) **377**, 606 (1995).
[5] S. P. D. Mangles *et al.*, Nature (London) **431**, 535 (2004).
[6] C. G. R. Geddes *et al.*, Nature (London) **431**, 538 (2004).
[7] J. Faure *et al.*, Nature (London) **431**, 541 (2004).
[8] W. Lu *et al.*, Phys. Rev. ST Accel. Beams **10**, 061301 (2007).
[9] A. G. R. Thomas *et al.*, Phys. Rev. Lett. **98**, 095004 (2007).
[10] G. Z. Sun *et al.*, Phys. Fluids **30**, 526 (1987).
[11] F. S. Tsung *et al.*, Phys. Rev. Lett. **93**, 185002 (2004).
[12] T. P. Rowlands-Rees *et al.*, Phys. Rev. Lett. **100**, 105005 (2008).
[13] W. Lu *et al.*, Phys. Rev. Lett. **96**, 165002 (2006).
[14] A. Pukhov *et al.*, Appl. Phys. B **74**, 355 (2002).
[15] P. Maurer *et al.*, arXiv:0906.1195v1.
[16] S. P. D. Mangles *et al.*, IEEE Trans. Plasma Sci. **36**, 1715 (2008).
[17] C. T. Hsieh *et al.*, Phys. Rev. Lett. **96**, 095001 (2006).
[18] J. Faure *et al.*, Nature (London) **444**, 737 (2006).
[19] J. Faure *et al.*, Phys. Rev. Lett. **95**, 205003 (2005).
[20] C. D. Murphy *et al.*, Phys. Plasmas **13**, 033108 (2006).
[21] R. A. Fonseca, *Lecture Notes in Computer Science* (Springer, Heidelberg, 2002), Vol. III-342, p. 2329.
[22] D. Umstadter *et al.*, Phys. Rev. Lett. **76**, 2073 (1996).
[23] A. Rousse *et al.*, Phys. Rev. Lett. **93**, 135005 (2004).
[24] S. Kneip *et al.*, Phys. Rev. Lett. **100**, 105006 (2008).